

# Phase and amplitude control of a multimode LMA fiber beam by use of digital holography

M. Paurisse<sup>1\*</sup>, M. Hanna<sup>1</sup>, F. Druon<sup>1</sup>, P. Georges<sup>1</sup>, C. Bellanger<sup>2</sup>, A. Brignon<sup>2</sup> and J. P. Huignard<sup>2</sup>

<sup>1</sup>Laboratoire Charles Fabry de l'Institut d'Optique, Campus Polytechnique, RD. 128  
91127 Palaiseau Cedex, France

<sup>2</sup>Thales Research and Technology, Campus Polytechnique, 1 Avenue Augustin Fresnel  
91767 Palaiseau Cedex, France

\*mathieu.paurisse@institutoptique.fr

**Abstract:** Amplitude and phase control of the output beam of a multimode LMA fiber supporting 4 modes is demonstrated by digital holography in both continuous and ns pulsed regimes at 1064 nm. Our system allows dynamic compensation of beam pointing instabilities, external perturbations introducing low order aberrations and fluctuations of the relative phase of the modes supported by the fiber.

©2009 Optical Society of America

**OCIS codes:** (060.2320) Fiber optics amplifiers and oscillators; (090.1995) Digital Holography; (060.5060) Phase modulation

---

## References and links

1. C. X. Yu, J. E. Kinsky, S. E. J. Shaw, D. V. Murphy, and C. Higgs, "Coherent beam combining of large number of PM fibres in 2-D fibre array," *Electron. Lett.* **42**(18), 1024–1025 (2006).
  2. J. Anderegg, S. Brosnan, E. Cheung, P. Epp, D. Hammons, H. Komine, M. Weber, and A. M. Wickham, "Coherently Coupled High Power Fiber Arrays," *Proc. SPIE*, **6102**, (2006).
  3. E. C. Cheung, M. Weber, and R. R. Rice, "Phase Locking of a Pulsed Fiber Amplifier," in *Advanced Solid-State Photonics*, Technical Digest (Optical Society of America, 2008), paper WA2.
  4. L. Lombard, A. Brignon, J. P. Huignard, E. Lallier, and P. Georges, "Beam cleanup in a self-aligned gradient-index Brillouin cavity for high-power multimode fiber amplifiers," *Opt. Lett.* **31**(2), 158–160 (2006).
  5. B. Steinhäusser, A. Brignon, E. Lallier, J. P. Huignard, and P. Georges, "High energy, single-mode, narrow-linewidth fiber laser source using stimulated Brillouin scattering beam cleanup," *Opt. Express* **15**(10), 6464–6469 (2007).
  6. C. Bellanger, A. Brignon, J. Colineau, and J. P. Huignard, "Coherent fiber combining by digital holography," *Opt. Lett.* **33**(24), 2937–2939 (2008).
  7. A. Brignon, L. Loiseau, C. Lara, J. P. Huignard, and J. P. Pocholle, "Phase conjugation in a continuous-wave diode-pumped Nd:YVO4 laser," *Appl. Phys. B* **69**(2), 159–162 (1999).
  8. W. Joseph, Goodman, *Introduction to Fourier Optics* (Roberts & Company Publishers, Englewood, 2005), Chap. 9.
  9. A. Sennaroglu, and J. G. Fujimoto, "Design criteria for Herriott-type multi-pass cavities for ultrashort pulse lasers," *Opt. Express* **11**(9), 1106–1113 (2003).
  10. I. Hartl, A. Marcinkevicius, H. A. McKay, L. Dong, and M. E. Fermann, "Coherent beam combination using multi-core leakage-channel fibers," in *Advanced Solid-State Photonics*, Technical Digest (Optical Society of America, 2009), paper TuA6.
- 

## 1. Introduction

Fiber lasers and amplifiers are very attractive for reaching high output powers because of their advantages in terms of compactness, efficiency, and thermal behavior. Unfortunately, the output power of such devices is limited by nonlinear effects and material damage, especially in the pulsed regime. To overcome this problem, increasing the effective area of the fibers is desirable, but this approach is limited because as the effective area is increased, the fiber supports higher order modes which degrade the output beam quality.

In order to scale the energy of pulsed fiber-based sources, a widely studied solution is coherent combining of several singlemode fiber amplifiers. This technique consists in locking different emitters in phase in order to add them coherently in the far-field. This results in an interference pattern composed of a sharp central lobe. Active coherent combining implies that the phase shift between the emitters is measured and compensated by phase modulators.

Excellent results have been obtained which led to a high number of coupled emitters [1], high power in the CW regime [2] and a first demonstration in the pulsed [3] regime. These techniques require either a complex phase determination of the output wavefront and/or iterative algorithms that makes the scaling to a high number of emitters non trivial.

Another way to scale the output power of fiber sources is to use a large area multimode fiber amplifier combined with a beam cleanup technique at the output to restore the spatial quality of the beam. For instance, stimulated Brillouin scattering (SBS) in a single multimode fiber has been used successfully to achieve beam cleanup, both in fiber lasers [4] and amplifiers [5]. However, this may introduce additional losses after the power amplification stage, and it is not adapted to the ns pulse regime since SBS requires narrowband signals.

Recently, an interesting coherent combining solution based on digital holography has been proposed and demonstrated with three passive single mode fibers [6]. This method builds upon phase conjugation techniques that are used in high power bulk lasers [7]. In this paper, we apply the digital holography concept to combine coherently the modes of a passive multimode large-mode-area (LMA) fiber. This can be viewed both as a control of the modal distribution in amplitude and phase inside a multimode fiber to obtain a flat-phase wavefront at the output, or as a beam cleanup technique performed before the injection. The implementation of the technique for a multimode fiber is more delicate than for several single mode fibers because it requires a true phase conjugation, as opposed to the compensation of constant phase shifts over otherwise plane waves. The advantage of such an architecture compared to one based on separate emitters is that the phase variation of modes inside the fiber are strongly correlated, which makes the entire system less sensitive to global phase fluctuations, such as temperature variations. Furthermore, the effective area is scaled using a fully monolithic amplifying medium, in contrast with conventional fiber beam combining. The self active phase compensation provided by digital holography allows compensating for relative phase fluctuations between the modes, due to external perturbations, without using iterative algorithms, and can be applied to any complex guiding structure, such as multi-core fibers (strongly coupled or not). We first present the principle of wavefront correction by digital holography in the context of a single multimode guiding structure, and demonstrate it both in the CW and nanosecond pulse regime. In such conditions, the corrected beam exiting the multimode fiber exhibits a Gaussian like intensity profile.

## 2. Digital holography principle and experimental setup

### 2.1 Principle of phase conjugation by digital holography

The principle of phase conjugation by digital holography is presented in Fig. 1. When a laser beam with a plane wavefront  $\varphi_{in}$  passes through an aberrating medium such as a multimode fiber, it acquires a spatial phase  $\varphi(x,y)$ , leading to a distorted wavefront and a poor spatial quality. This process can be described as follows: the injected Gaussian beam is decomposed on the modes  $E_{LPnm}$  of the fiber:

$$E_{input}(x, y) = \sum_{nm} c_{nm} E_{LPnm}(x, y) \quad (1)$$

where  $E_{LPnm}$  is the field of the mode  $LP_{nm}$  of the fiber, and  $c_{nm}$  are defined as:

$$c_{nm} = \frac{\left( \iint E_{input}(x, y) \cdot E_{LPnm}^*(x, y) \cdot dx \cdot dy \right)^2}{\left( \iint E_{input}(x, y) \cdot dx \cdot dy \right)^2 \left( \iint E_{LPnm}(x, y) \cdot dx \cdot dy \right)^2} \quad (2)$$

These modes propagate along the fiber and interfere during propagation, which leads to an object beam with a distorted wavefront at the output of the fiber  $O(x,y)$ .

$$O(x, y) = \sum_{nm} c_{nm} E_{LPnm}(x, y) \cdot e^{i\beta_{nm}L} \quad (3)$$

where  $\beta_{nm}$  is the propagation constant of the mode  $LP_{nm}$  and  $L$  is the length of the fiber.

To generate the phase conjugate of  $O(x,y)$ , an interference pattern between this beam and a reference beam with a plane wavefront  $\varphi_R$  is recorded on a CCD camera and displayed onto a spatial light modulator (SLM), thus forming a holographic diffraction pattern. A fraction of the reference beam is sent on this diffraction pattern, which results in the Raman-Nath regime in the formation of three main diffraction orders: the 0 order, resulting from the reflection of the reference beam on the surface of the SLM, the +1 order, which is proportional to  $O(x,y)$ , and the -1 order, proportional to  $O^*(x,y)$  [8].

By injecting the -1 order into the fiber, the same set of modes that the one composing  $O(x,y)$  is excited, but with a conjugated phase for each mode:

$$E_{reinjected} = O(x,y)^* = \sum_{nm} c_{nm} E_{LPnm}^*(x,y) e^{-i\beta_{nm}L} \quad (4)$$

As the reinjected beam propagates back through the fiber, each mode acquires a phase delay of  $e^{i\beta_{nm}L}$ , which cancels the initial phase term, leading to a corrected beam with a plane wavefront  $\varphi_{out}$ .

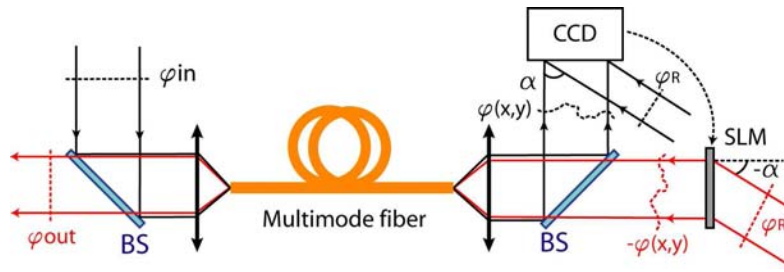


Fig. 1. Principle of wavefront correction by digital holography. SLM, spatial light modulator; BS, beamsplitter

If the reference beam and the object beam are tilted with an angle  $\alpha$  when the interference pattern is recorded, the three orders of diffraction are separated angularly. The -1 order is diffracted with an angle  $-\alpha$ , and the +1 order with an angle  $\alpha$ . This can be used to discriminate the two orders of diffraction. Although the principle is presented with an SLM in transmission for clarity, the actual component used in the experiment is reflective.

## 2.2 Description of the experimental setup

The experimental setup used to perform wavefront control of a multimode LMA fiber is shown in Fig. 2. The laser source is either continuous or pulsed at 1064 nm and will be described in Sections 3 and 4. The Gaussian beam emitted by the laser is expanded with a telescope to reach 3 mm diameter so as to minimize its divergence. Beamsplitter BS1 splits the beam into a beam which will be injected into the LMA fiber with a 30 mm focal length lens L1, and the reference beam. The LMA fiber is 3 m long, has a 20  $\mu\text{m}$  core diameter, supports 4 modes and is polarization maintaining (PM). It is not coiled and the size of the injected beam is not adapted to the fundamental mode on purpose to excite several modes. As several modes are excited during propagation, the total effective area of the beam is larger than in the fundamental case. The end facet of the fiber is imaged onto CCD 1 with the 18 mm focal length lens L2.

An adjustable delay line can be inserted when the pulsed laser source is used, to compensate for the low coherence length of the laser. The reference beam and the object beam are tilted by a small angle  $\alpha$  and an interference pattern is recorded on CCD 1. This interference pattern consists in fringes which are not equally spaced due to the relative phase difference between the reference beam and the superposition of the excited modes of the fiber. The interference pattern obtained is then displayed onto a phase only SLM via a computer, which creates a dynamic digital holographic diffraction pattern. The SLM is positioned at the same distance from BS3 as CCD 1. A fraction of the reference wave is sent on the SLM via

BS3 and diffracts on the hologram. The +1 and -1 orders are separated angularly by an angle  $\alpha$  from both sides of the 0 order [8].

The output beam is recorded on CCD 2 and has the same spatial characteristics as the input beam  $E_{input}$  which has a plane wavefront.

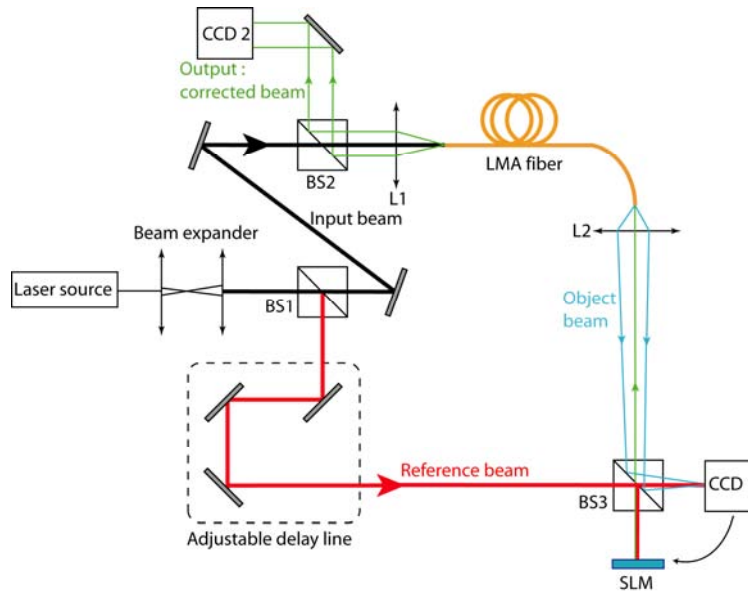


Fig. 2. Experimental setup. SLM, spatial light modulator; BS, beamsplitter; L, lens.

### 2.3 Experimental procedures and discussion

The exact conjugate of the object beam has to be created by the hologram to ensure good fidelity phase conjugation. To do that, the linearity between the interference pattern and the displayed hologram has to be controlled. The CCD camera (CCD 1) used to record the interference pattern is a Spiricon Laser Beam Analyzer which software displays a linear image on the computer. This image is directly displayed on the SLM without any additional treatment. The SLM used is a reflective phase only liquid crystal on silicium (LCOS) manufactured by Holoeye which can perform up to  $2\pi$  linear phase shift at 1064 nm, has a 1920x1080 resolution, and a pixel size of 8  $\mu\text{m}$ . The size of the reconstructed object beam has also to be precisely controlled. Indeed, as opposed to traditional holography, the recording and the reading media are separate. The resolution of the CCD is different from the one of the SLM, which leads to a magnification of the image displayed on the SLM. The size of the displayed image is adjusted to perform exact size matching with the object beam.

The measured diffraction efficiency on the hologram displayed on the SLM is about 1% in the following experiments. This relatively low value has two causes. First, the reference was chosen larger than the object beam to make the alignment of the two beams easier. Therefore, the part of the reference beam which does not interfere with the object beam is not diffracted, which reduces the efficiency. In addition, the number of pixels of the SLM per fringes of the interference pattern is low (about 10) and limits the diffraction efficiency. This is due to the fact that the end facet of the fiber is imaged onto CCD 1 and thus is quite small. Working in a defocused situation or in the far-field is a simple solution to increase this diffraction efficiency. Yet, the experiments presented below are proof on principle experiments, and working in the near-field allows seeing more clearly the structure of the object beam and the changes in the hologram.

Reinjection is also a crucial issue to perform phase conjugation. For that purpose, the SLM is mounted on a kinematic mirror mount to control the injection angle. The position of the

injected beam is directly controlled by moving the hologram on the SLM. With these two parameters, coupling was optimized to maximize the output power.

The precision of the displayed phase and the speed of the correction are two important parameters for active phase control. The precision of the phase control is determined by the number of pixel of the CCD composing the fringes spacing. Indeed, a number  $d$  of pixels composing the fringe spacing ensures a phase control of  $\lambda/d$  [6]. In our case, the fringe spacing was about 20 pixels, resulting in a potential phase control precision of  $\lambda/20$ . Increasing the number of pixels by reducing the angle between the reference beam and the object beam would allow better precision. But on the other hand it would also reduce the diffraction angle, making the reinjection of the  $-1$  order only more difficult.

The speed of the correction is limited in our experiment by the camera which had a bandwidth of 12 Hz at full resolution (1616x1216, 16 bits). This bandwidth is sufficient to compensate for thermal variations (see Section 3) but not to compensate for vibrations on the table. This low value is imposed by the high resolution of the camera and by the USB connection. By decreasing the resolution and using a FireWire connection, a bandwidth of 60 Hz is possible. In our experiment, the upper limit is imposed by the SLM which works at 60 Hz. Higher bandwidth correction implies the use of other SLM technologies, such as micro-mirror arrays which can work at frequencies up to 5 kHz.

### 3. Experimental results with the continuous laser source

The experimental setup described above was first tested with a single longitudinal mode Nd:YAG CW laser source. The laser had a spectral narrow linewidth below 1 kHz, which ensured a long enough coherence length to get interferences on CCD 1 and at the output without a delay line. To get interferences at the output, the experimental setup was modified as shown in Fig. 3.

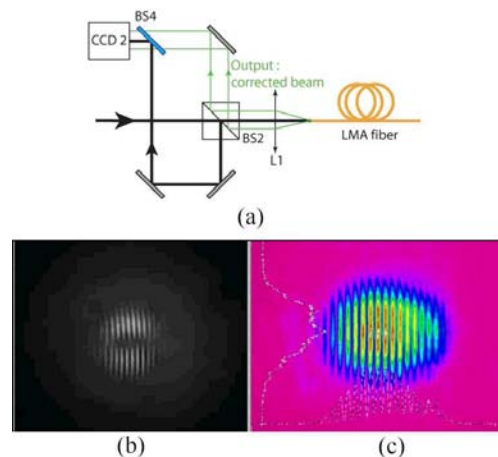


Fig. 3. Influence of thermal heating of the fiber on phase conjugation ([Media 1](#)). (a) Modified output of the experimental setup. (b) Recorded hologram on CCD 1. (c) Interference pattern between the output beam and the reference beam on CCD 3.

A fraction of the beam coming from the laser source is sent on CCD 2 via BS2 and an interference pattern between this beam and the output beam is recorded on CCD 2 via BS4. This was used to verify that phase conjugation could be achieved: by heating the fiber with a lamp, a global phase that varies with time is added to the object beam, making the fringe pattern move. If the  $-1$  order is coupled to the fiber, the output beam should be phase locked to the reference. In such operation, the holographic fringes displayed on the SLM are self-adjusted such that the interference pattern between the reference beam and the output beam on CCD 2 is fixed. [Media 1](#) shows a video of these output fringes. First, a fixed interference pattern is recorded and displayed on the SLM (image (b) of Fig. 3). At the output, an

interference pattern is also recorded on CCD 2 (image (c)). At a certain point, a lamp is turned on to heat the fiber, which can be seen on the change of background of the right image in [Media 1](#). Since the hologram is fixed, there is no phase compensation and the fringes at the output begin to move. Then, the active phase correction is turned on, making the fringes of the hologram move. As a result, the fringes at the output stop moving, as the output beam is now phase-locked to the reference beam.

To demonstrate the system ability to maintain fundamental mode operation when an external phase perturbation is applied, we inserted a 500 mm focal length lens tilted at about 40 degrees outside the fiber between L2 and BS3 which introduced some focus and low frequency aberrations. Figure 4 shows that we were able to compensate to a large extent the phase error introduced by the lens, without correcting the injection in the fiber.

First, an interference pattern is recorded on CCD 1 (image (a)) and is displayed on the SLM. The reference beam diffracts on this holographic pattern and the  $-1$  order is reinjected in the fiber. The corrected beam is recorded on CCD 2 (image (b)). The hologram is then frozen, by pausing the CCD 1 and the tilted lens is inserted. As the recorded hologram is fixed, it cannot compensate for the amplitude and phase distortion introduced by the lens and the reinjected beam is not corrected anymore on CCD 2, as shown on image (c). A new hologram corresponding to the superposition of the distorted wavefront exiting the fiber and the distortion introduced by the lens is then recorded on CCD 1 (image (d)). As a result, a  $-1$  order with different amplitude and phase profiles is created and reinjected into the fiber, and a corrected output beam can be recorded on CCD 2 (image (e)).

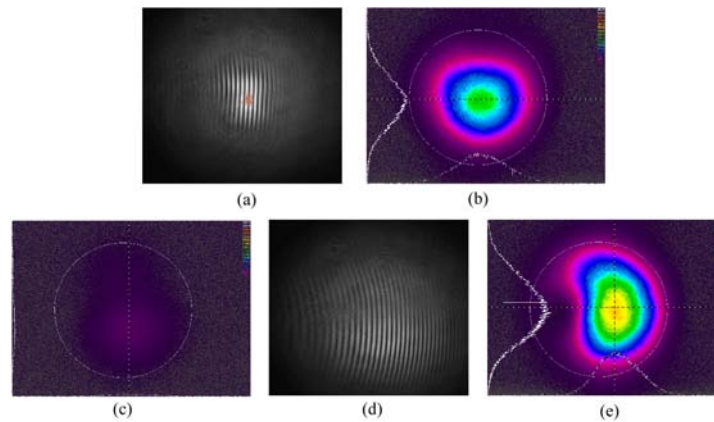


Fig. 4. Compensation of the phase error introduced by a 500 mm focal tilted lens. (a) Recorded hologram on CCD 1 without lens. (b) Corresponding output beam on CCD 2. (c) Output beam on CCD 2 after the insertion of the lens without changing the hologram. (d) New recorded hologram after the insertion of the lens. (e) Corresponding output beam on CCD 2.

The difference between images (b) and (e) is due to the fact that the lens also induces a magnification of the object beam on CCD 1 which becomes larger than the reference beam. As a consequence, the outer part of the object beam does not interfere with the reference beam and information about the wavefront is lost. The reconstructed beam is then slightly different from  $O(x,y)^*$  and exact phase conjugation is not achieved. This experiment also showed the influence of incomplete phase compensation on the beam quality. This defect can be corrected by increasing further the size of the reference beam, ultimately limited by the SLM size.

A similar experimental setup can be used to verify the sensitivity of our system to misalignment, by inserting a thick tilted plane plate instead of the tilted lens. The images presented in Fig. 5. show that our system is insensitive to beam pointing instabilities up to a certain angle imposed by the size of the reference beam.



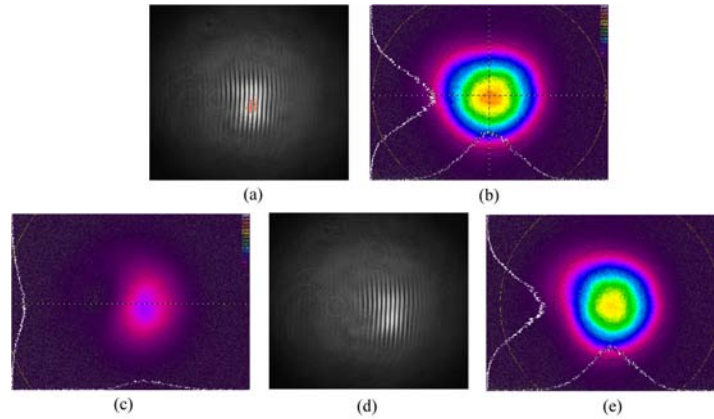


Fig. 5. Sensitivity to misalignment. (a) Recorded hologram on CCD 1 without plane plate. (b) Corresponding output beam on CCD 2. (c) Output beam on CCD 2 after the insertion of the plate without changing the hologram. (d) New recorded hologram after the insertion of the plate. (e) Corresponding output beam on CCD 2.

The results presented above show that the system is able to compensate external phase errors such as aberrations and beam displacement. However these compensations are limited by the limited size of the reference beam. A relative phase change between the modes does not lead to an image magnification or a displacement of the beam, but changes the intensity and phase pattern of the object beam. To study this point, we applied a local pressure to the fiber. The pressure is weak to limit the induced losses in the fiber but strong enough to observe a drastic change of the intensity distribution at the output of the first pass in the fiber. The results are shown in Fig. 6.

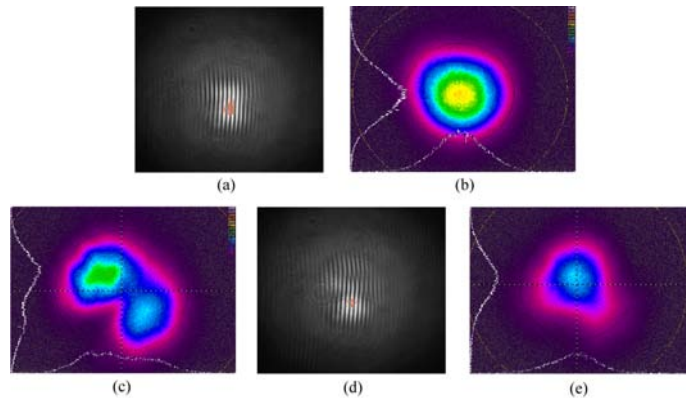


Fig. 6. Application of a pressure to the fiber. (a) Recorded hologram on CCD 1 without pressure. (b) Corresponding output beam on CCD 2. (c) Output beam on CCD 2 with a pressure applied. (d) New recorded hologram after the application of the pressure. (e) Corresponding output beam on CCD 2.

We observed a significant improvement of the quality of the output beam when the active correction was applied, as it switched from a bi-lobe mode to a single lobe one. Yet we observed a decrease in the coupled power and we were also unable to achieve exact phase conjugation as it can be seen by the difference between images (b) and (e). This can be explained by two reasons. First, the pressure introduces losses which cannot be compensated by the hologram. The losses are not negligible as the power of the object beam dropped from 3.6 mW to 2.6 mW after the application of the pressure. Second, there is a pressure-induced modification of the polarization state, even for this PM fiber. We observed that the beam was 92% polarized when no pressure is applied, and this value decreased with the intensity of the

pressure, reaching 81% in the case of the images shown in Fig. 6. This problem will not appear if only the relative phase between the modes changes.

#### 4. Experimental results with the pulsed laser source

The primary application of coherent modal combining in multimode fiber is pulse amplification with active doped fiber in order to overcome peak power limitations observed in single mode fibers. Here, we demonstrate that the digital holography technique is compatible with a pulsed laser source. The laser delivers 1 ns pulses with a 40 kHz repetition rate at 1064 nm, and an average power of 250 mW. A delay line is introduced in the reference arm of the interferometer to compensate for the delay between the reference pulse and the object pulse, due to the 3 m long fiber. The delay line is in a 3-m q-preserving double pass geometry composed of a plane mirror and a concave mirror with 1.5 m radius of curvature, separated by a distance of 0.75 m [9]. The optimal delay is obtained by inserting a retro-reflector mounted on a translation stage before the q-preserving cavity. This allows a precise optimization of the hologram interference contrast. As in the case of the CW source, we studied the response of the system to the application of a pressure in the fiber, as shown in Fig. 7.

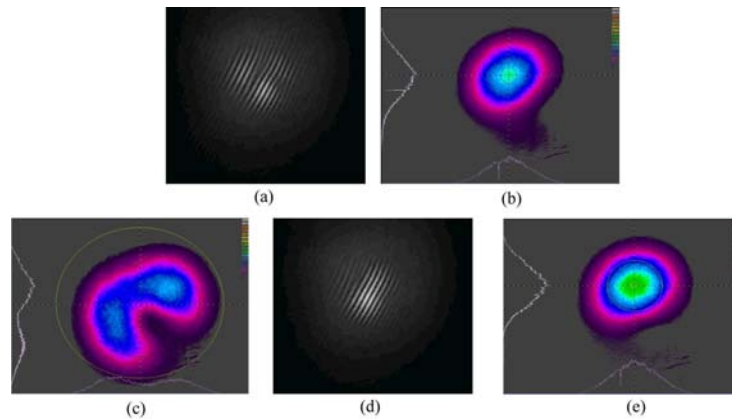


Fig. 7. Application of a pressure to the fiber in the pulsed regime, frame excerpts from Media 2. (a) Recorded hologram on CCD 1 without pressure. (b) Corresponding output beam on CCD 2. (c) Output beam on CCD 2 with a pressure applied. (d) New recorded hologram after the application of the pressure. (e) Corresponding output beam on CCD 2.

The dynamic response of the system can also be seen in Media 2. Like in the case of the CW regime, a good correction of the beam is observed. The correction is once again limited by the losses and the rotation of the polarization induced by the pressure. We measured the spatial quality of the corrected beam, resulting in  $M^2$  parameters of 1.2 and 1.1 in the x and y directions respectively.

An advantage of this setup for the wavefront correction of laser pulses is that no phase measurement is needed, since it is automatically performed by the holographic diffraction pattern. There is no need either of an iterative algorithm to determine the phase pattern that should be introduced. However, because of the digital nature of the holography, we retain some control over the phase compensation by using image processing between the CCD image and the SLM-displayed image, for example contrast enhancing might be useful in some situations.

#### 5. Conclusion

Amplitude and phase correction by digital holography in a 20  $\mu\text{m}$  core diameter multimode LMA fiber has been demonstrated for both continuous and nanosecond pulsed regimes. As the beam is decomposed on higher order modes while it propagates along the fiber, an increase of the effective area is obtained with a standard fiber design. Contrary to multimode interference techniques, no control is needed on the length of the fiber. Our system showed efficient



correction of beam pointing instabilities, low aberrations introduction, and relative phase change between the modes. The absence of any feedback loop algorithm to recover the phase ensures a fast active correction (limited in our case by the frame rate of the camera for the hologram acquisition) and is particularly adapted for the case of pulsed regimes.

Our technique is also applicable to active fibers and other multimode structures. An interesting alternative is to use multi-core fibers, since it was shown that relative phase fluctuations are reduced due to the geometrical proximity of the cores [10]. Our primary studies performed on a 19 cores multi-core fiber have shown that depolarization is limited in such structures, allowing the efficient use of phase compensation by digital holography technique.

### **Acknowledgments**

The authors thank the Manolia group from the Laboratoire Charles Fabry de l'Institut d'Optique for the loan of the CW monomode longitudinal laser. M. Paurisse acknowledges the funding of his PhD by the French Délégation Générale de l'Armement.